Integrating boron atoms into ultrathin organic polymer for visible light photocatalytic CO_2 reduction to CH_4 with near 100%

Linquan Hou[a,1], Guoen Tang[a,1], Hao Huang[a], Shiheng Yin[b], Bei long[a], Atif Ali[c], Guo-Jun Deng[a], Ting Song[a*]

a Key Laboratory for Green Organic Synthesis and Application of Hunan Province, Key Laboratory of Environmentally Friendly Chemistry and Application of Ministry of Education, College of Chemistry, Xiangtan University, Xiangtan 411105, P. R. China.

b Analytical and Testing Center, South China University of Technology, Guangzhou 510640, P. R. China.

c Department of Chemistry and State Key Laboratory of Synthetic Chemistry, The University of Hong Kong, Pokfulam Road, Hong Kong, P. R. China.

1These authors contribute equally to this work.

*Corresponding author. E-mail: songtg@xtu.edu.cn

Computational methods

The first-principles calculations based on the Density Functional Theory (DFT) were performed using the Materails Studio software with CASTEP model. The Perdew-Burke-Ernzerhof (PBE) exchange-correlation functional within the generalized gradient approximation (GGA) was employed to describe the exchange-correlation energy. The energy cutoff for the plane wave basis expansion was set to 600 eV. The force on each atom was set as 0.03 eV/Å for convergence criterion. Slab model was constructed in a 4×4 supercell, with a vacuum layer of 20 Å in the z direction to avoid the interaction between layers. The sampling in the Brillouin zone was set with 3×3×1 by the Monkhorst-Pack method. The van der Waals interaction was considered by using DFT-D3 method. The free energies of the CO_2 reduction reaction steps were calculated using the equation: $\Delta G = \Delta E_{DFT} + \Delta E_{ZPE} - T\Delta S$ where ΔE_{DFT} is the DFT energy difference, the ΔE_{ZPE} and $T\Delta S$ are the zero-point energy correction and the variation of entropy, respectively, which gotten from vibration calculations. Moreover, the ΔE_{ZPE} and $T\Delta S$ of molecules in the gas phase were taken from the NIST database.

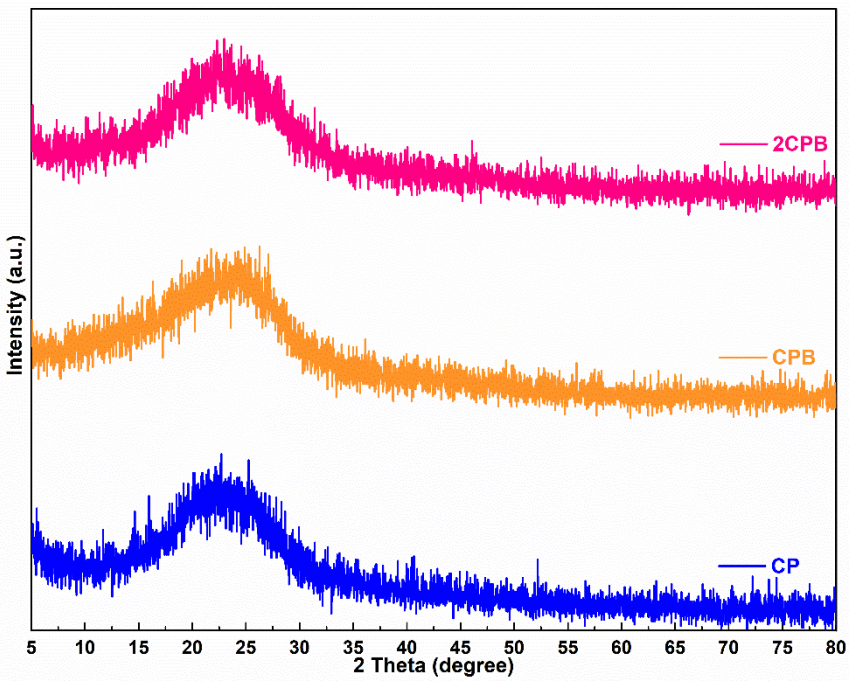

Fig. S1 XRD patterns of CP, CPB and 2CPB samples.

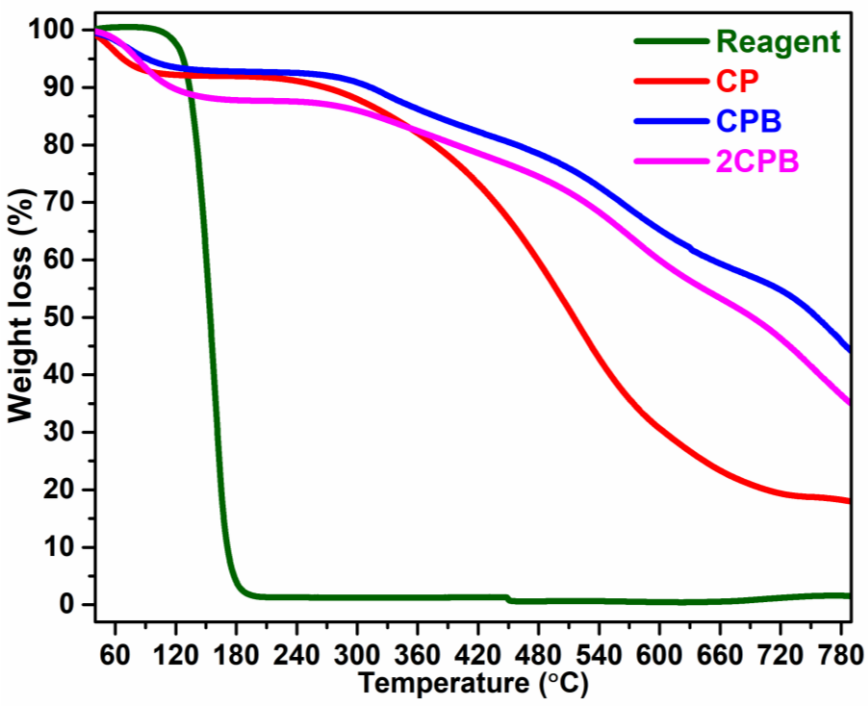

Fig. S2 Thermogravimetric analysis results of reagent (phosphonitrilic chloride trimer), CP, CPB and 2CPB samples.

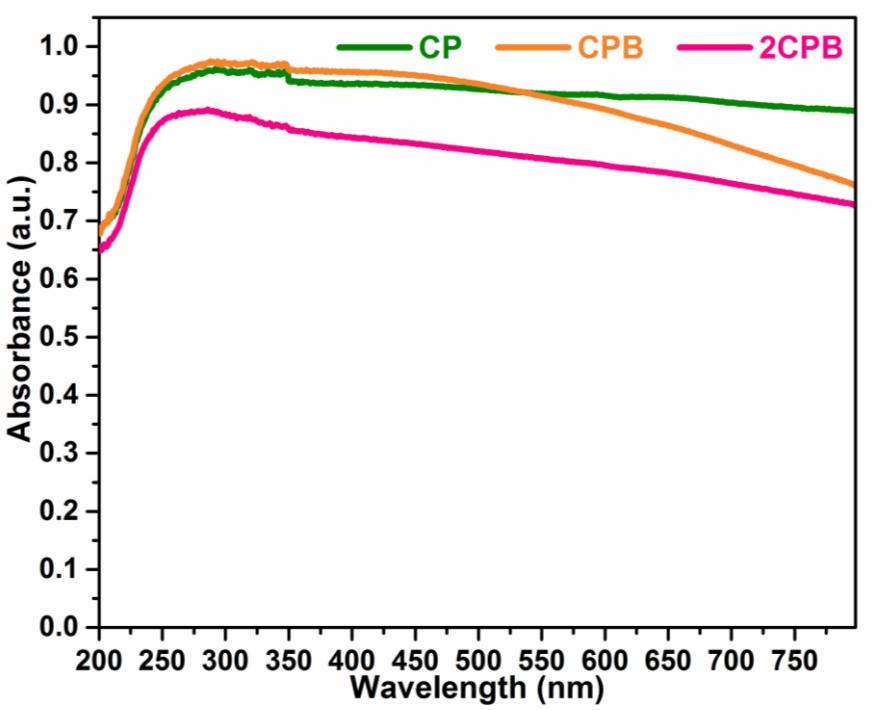

Fig. S3 UV-vis diffuse reflectance spectra (DRS) of CP, CPB and 2CPB samples.

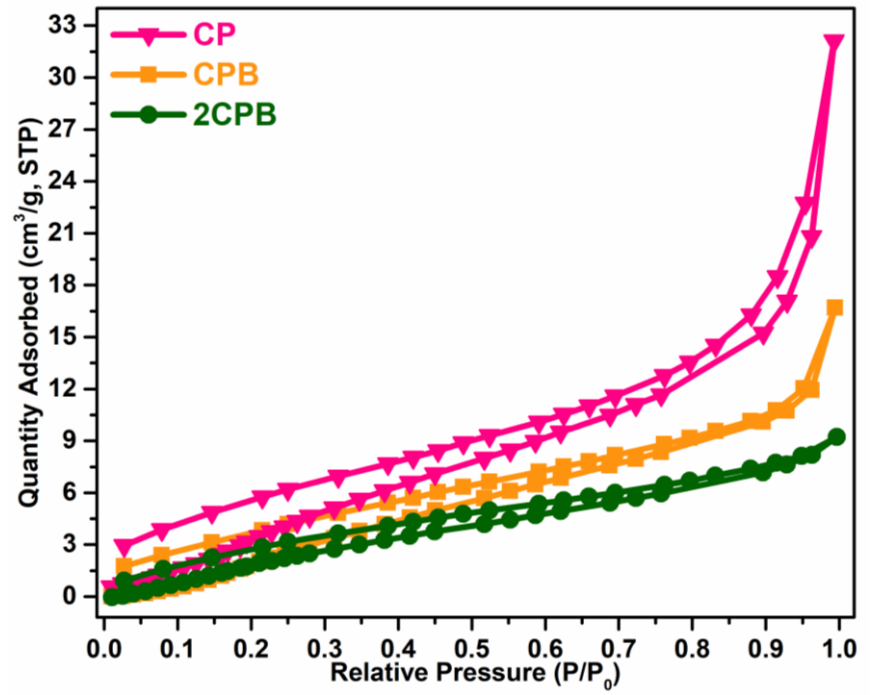

Fig. S4 N_2 adsorption-desorption isotherms at 77 K of CP, CPB and 2CPB samples.

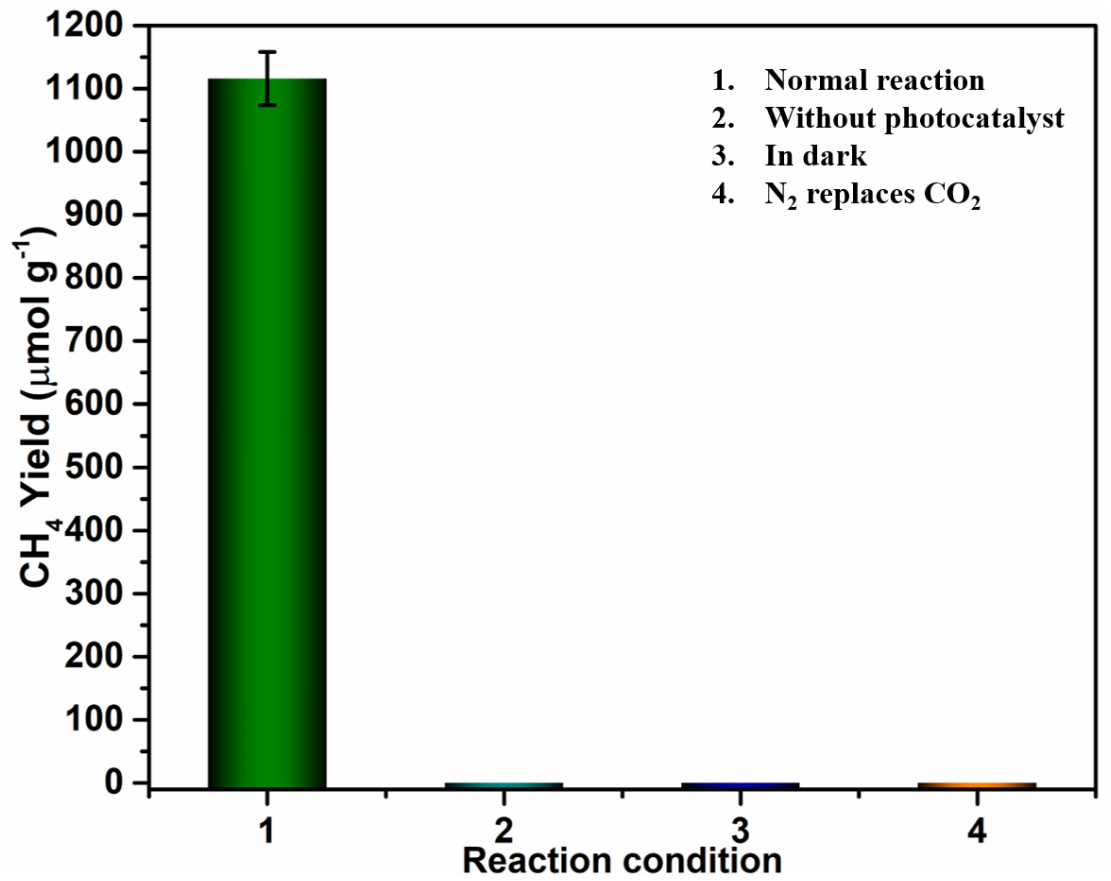

Fig. S5 CH_4 yield of CPB sample under various reaction conditions.

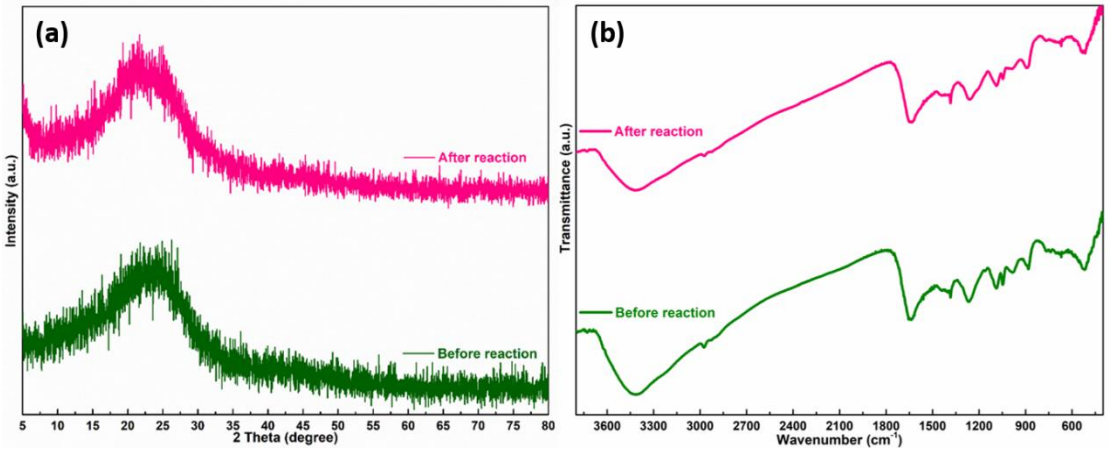

Fig. S6 XRD patterns (a) and fourier transform infrared spectra (b) of CPB sample before and after the stability test.

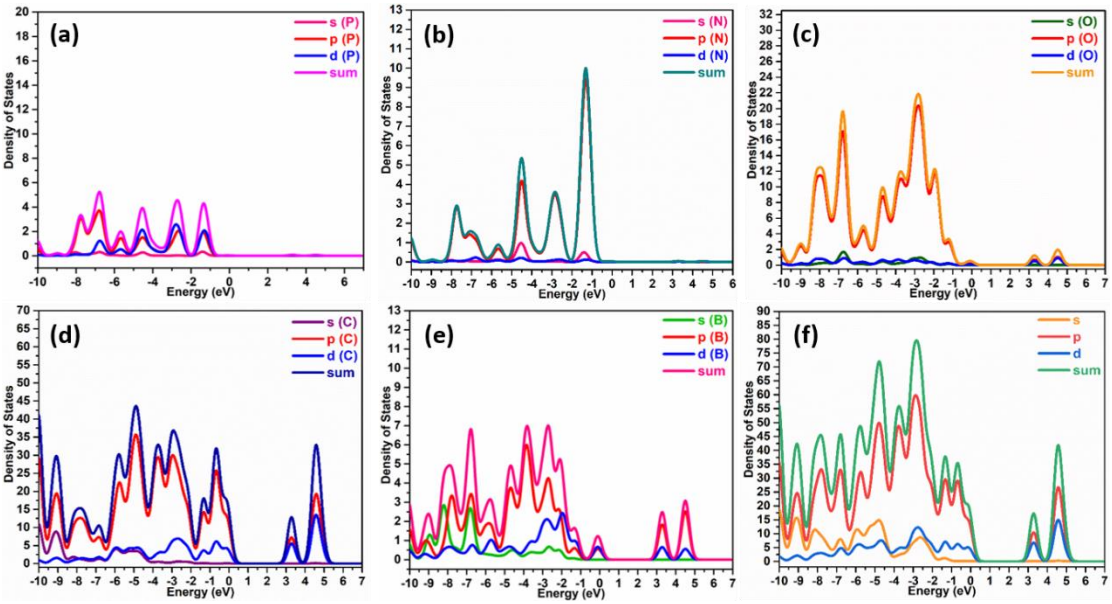

Fig. S7 Calculated partial density of states of (a-e) CPB, while (f) represents the total density of states of CPB.

Table S1. The comparation of photocatalytic CO_2 reduction activity among some representative photocatalysts reported in the literatures over recent years and ***this work***.

Photocatalyst	CH_4 evolution rate ($\mu mol\ g^{-1}\ h^{-1}$)	Light source	CH_4 Selectivity	Ref.
Metal-free CPB	1115.8 μmol g^{-1} (5 h)	300 W Xe lamp ($\lambda \geq 420$ nm)	>99%	**This work**
Cu_3SnS_4	22.6	300 W Xe lamp ($\lambda \geq 420$ nm)	83%	[1]
Ni-MoP@NC_{PF}	9.78	350 W Xe lamp (420 nm filter)	1%	[2]
CoNiSx-CN	0.9	350 W Xe lamp	10%	[3]
Au/CDT-DCDA-490	9.7	300 W Xe lamp (420 nm filter)	13%	[4]
NH_2-UiO-66/$CdIn_2S_4$	2.9	300 W Hg lamp ($\lambda \geq 420$ nm)	20%	[5]
TiO_2/$MoSe_2$	50	300 W Xe lamp	57%	[6]
WO_3 QDs/$CdIn_2S_4$	1.6	350 W Xe lamp ($\lambda \geq 420$ nm)	17%	[7]
g-C_3N_4@$CuIn_5S_8$	4.8	300 W Xe lamp ($\lambda \geq 420$ nm)	73%	[8]
Environmental phosphorylation	6.0	350W Xe lamp	5%	[9]
V_O-In_2O_3	0.8	300W Xe lamp $\lambda > 400$ nm	1.8%	[10]
$FAPbBr_3$/α-Fe_2O_3	10.5	300 W Xe lamp ($\lambda \geq 400$ nm)	21%	[11]
Zn_2GeO_4:Er^{3+}/g-C_3N_4	11	300 W Xe lamp	13%	[12]
Co/MXene-NH_3	30.4	300 W Xe lamp	86%	[13]
$Cs_3Sb_2I_9$	4.5	300 W Xe lamp	5%	[14]
TiO_2@TiO_{2-x}	3.5	300 W Xe lamp (Visible light)	77%	[15]

References

[1] J. Y. Wang, T. T. Bo, B. Y. Shao, Y. Z. Zhang, L. X. Jia, X. Tan, W. Zhou, T. Yu, Appl. Catal. B: Environ. 297 (2021) 120498.

[2] S. Q. Gong, M. J. Hou, Y. L. Niu, X. Teng, X. Liu, M. Z. Xu, C. Xu, V. Ka-Man Au, Z. F. Chen, Chem. Eng. J. 427 (2021) 131717.

[3] F. P. Li, Y. H. Huang, C.Y. Gao, X. Y. Wu. Mater. Res. Bull. 144 (2021) 111488.

[4] W. L. Zhen, J. J. Sun, X. F. Ning, X. Y. Shi, C. Xue, Appl. Catal. B: Environ. 298 (2021) 120568.

[5] L. F. Hong, R. T. Guo, Z. W. Zhang, Y. Yuan, X. Y. Ji, Z. D. Lin, W. G. Pan, J. CO_2 Utili. 51 (2021) 101650.

[6] S. H. Kang, H. T. Khan, C. H. Lee, K. J. Kwon, C. L. S. Y. Lee, Chem. Eng. J. 420(2021) 130496.

[7] Z. Z. Zhang, Y. X. Cao, F. H. Zhang, W. J. Li, Y. L. Li, H. Yu, M. Y. Wang, H. B Yu, Chem. Eng. J. 428 (2022) 131218.

[8] S. M. Liu, L. J. Chen, T. T. Liu, S. Cai, X. X. Zou, J. W. Jiang, Z. Y. Mei, Z. H. Gao, H. Guo, Chem. Eng. J. 424(2021) 130325.

[9] J. C. Wang, J. Wang, N. Y. Li, X. Y. Du, J. Ma, C. H. He, Z. Q. Li, ACS Appl. Mater. 12 (2020) 31477.

[10] X. W. Zhu, J. M. Yang, X. L. Zhu, J. J. Yuan, M. Zhou, X. J. She, Q. Yu, Y. H. Song, Y. B She, Y. J. Hua, H. M. Li, H. Xu, Chem. Eng. J. 422 (2021) 129888.

[11] Y. F. Mu, C. Zhang, M. R. Zhang, W. Zhang, M. Zhang, T. B. Lu, ACS Appl. Mater. Interfaces. 13 (2021) 22314.

[12] Z. Han, Y. Zhao, G. Gao, W. Zhang, Y. Qu, H. Zhu, Zhu, P. Wang G, Small 17 (2021) 2102089.

[13] J. Ma, Q. Jiang, Y. A. Zhou, W. Chu, S. Perathoner, C. F. Jiang, K. H. Wu, G. Centi, Y. F. Liu, Small 17 (2021) 2007509.

[14] Y. Y. Wang, Q. X. Zhou, Y. F. Zhu, D. S. Xu, Appl. Catal. B: Environ. 294 (2021) 120236.

[15] Q.Y. Bi, K. Y. Hu, J. C. Chen, Y. R. Zhang, M. S. Riaz, J. Xu, Y. F. Han, F. Q. Huang, Appl. Catal. B: Environ. 295 (2021) 120211.